INTERNATIONAL BUILDING PERFORMANCE SIMULATION ASSOCIATION ENGLAND

Proceedings of BSO-VI 2022
Sixth Building Simulation and Optimisation Virtual Conference
13 - 14 December 2022
Hosted by University of Bath, UK

Comparative analysis of daylight levels in an office space considering standard overcast sky condition and measured CIE sky type of Gurugram, India

Rohit Thakur[1], Riya Malhotra[1], Ankit Bhalla[2], Sanjay Seth[1]
[1] The Energy and Resources Institute, Delhi, India
[2] GRIHA Council, Delhi, India

Abstract

The climatological study of sky conditions and radiation is relatively new in India. Prediction of daylight availability in an interior space throughout the year is imperative for daylighting design. This prediction of daylight availability is made in absolute or relative terms to external illuminance. This paper aims to showcase the correlation analysis of the measured CIE sky and overcast Sky for equinox days; March 21 and September 21. VELUX daylight visualizer software were used to run a box model analysis to extract illuminance levels for a correlation study of observed CIE sky conditions with overcast sky conditions. From the correlation analysis of the simulated data, it is computed that the illuminance analysis perceived by daylight simulation considering measured sky conditions compared to overcast sky conditions on the analysis grid is 23% more accurate in March and 42% more accurate in September. Therefore, it can be affirmed that the computed set of CIE design skies shall be used to enhance the passive design of windows for the locations falling under the respective climatic zones for better cost optimization through accurate illuminance prediction.

Key Words

Daylight, Sky Patterns, CIE Sky Type

Introduction

In commercial buildings, daylighting efficiently produces a pleasant visual environment and is a significant source of energy savings. The daylight quality is the only light source closely resembling the visible human reaction, making it the most excellent light source for accurate colour depiction. The majority of daylight enters a building through window openings, which serve the dual purpose of bringing light inside to create a more beautiful and pleasant ambience and allowing occupants to keep an eye on the outside World. People want their workplaces to have adequate natural illumination [1]. To apply energy conservation measures and guarantee the interior environment's quality, it is crucial to define the overall design method for the thermal and luminous environment before integrating daylight into the structure [2-3]. The brightness levels and patterns of the Sky in the direction of view of the surface, the quantity and kind of daylight, buildings orientation, and the nearby buildings all impact the amount of daylight illumination within buildings at any time. The way daylight enters a building also relies on the type of building apertures [4-5].

Predicting daylight availability at the early design stage to best define and optimize the façade and fenestration is the first step in harnessing daylight efficiently and correctly for building design. The daylight factor (DF), the ratio of indoor illumination to the simultaneous illumination accessible on a horizontal plane from the entirety of an unobstructed sky, is traditionally used to assess daylighting efficiency [1]. The sky component (SC), the externally reflected component (ERC), and the internally reflected component (IRC) are separated into three parts for computing proposals (IRC). The idea of the split-flux principle, which splits the flux entering the interior through windows into its lower sections of the room surface areas and total internal surface areas, is the foundation for the computation of the average DF. The bigger the floor and interior room surface areas, the smaller will be the average DF. As a result, the Sky's brightness patterns and levels determine the inside daytime illuminance [6-7]. For determining the sky luminance distribution to predict indoor daylight illuminance, the availability of reliable meteorological data is essential. When evaluating the look and functionality of interior spaces, which are extremely sensitive to the dynamic brightness of the visible sector of the Sky, sky luminance is a crucial factor [8].

Several research on the distribution pattern of sky models is in the public domain. The 15 general sky types designated by the International Commission on Illumination (CIE) in France depict various sky circumstances [9]. These models aid in determining sky brightness in a variety of weather scenarios, from a clear to cloudy Sky. According to the literature analysis, researchers have sought to identify methodology and appropriate CIE sky types for some tropical nations, but no comparable in-depth study for India's tropical environment has been carried out. Furthermore, it appears that no widely disseminated research makes design suggestions for the passive design of windows for daylighting in tropical climates, given that Sky luminance varies depending on a number of difficult-to-specify meteorological, seasonal, and geometric parameters [10]. The exact measurements of the luminance data are necessary to determine the CIE sky type of any place. The daylight availability characteristics, measured globally in 1991 as part of the International Daylight Measurement Program (IDMP), included India. However, no measurements have been done since the data was last recorded in the IDMP. The unavailability of measured luminance data limits the use of the CIE sky model for passive window design in many countries.

CIE sky models are mathematical simulations that may be used to reproduce the luminance distributions of the Sky at different times of the day. The solar position, atmospheric turbidity, air pollution, cloud quantity, type, and pattern, which can alter unpredictable sunshine and skylight [11], are some elements that contribute to the sky brightness distributions and can only be determined from sky measurement data. Illuminance data are often advised to be gathered over a lengthy period to discover recurring patterns and eradicate irregularities to create CIE sky models and correctly complete daylight simulations.

The solar position is calculated using daylighting simulation software using the site's location (latitude and longitude), date, and simulation time. Most simulation programmes utilize CIE overcast or CIE clear sky as the input for the sky type. Although these extreme sky types are crucial for window design, they do not accurately reflect real-world situations in energy simulations. For instance, the SUPERLITE software creates the luminance distribution for a uniform sky, a CIE overcast sky, and a CIE clear sky with or without the sun. The gensky programme, a component of the RADIANCE package, also uses these sky conditions [10]. Although these extreme sky types are crucial for window design, they do not accurately reflect real-world situations in energy simulations. The standard methods are required for harmonies daylight design and daylighting consequences. The varied CIE sky conditions are also included in the VELUX Daylight Visualizer, although only for the 21st day of the month. At the moment, sophisticated computational tools like Rhino's grasshopper and other programming tools allow users to quickly create plug-ins to carry out numerous simulations and analyses. However, relatively few daylighting plug-ins take into account the distribution of the CIE 15 sky model. This paper seeks to understand how daylight levels in an office space vary, considering the measured CIE sky type against the standard overcast conditions.

TABLE I. A SET OF 15 STANDARD SKY TYPES AND THEIR PARAMETRIZATION (CIE, 2003)

Sky Type	Description of Sky
Sky Type 1	Overcast with steep gradation and azimuthal uniformity
Sky Type 2	Overcast with the steep gradation and slight brightening towards the sun
Sky Type 3	Overcast moderately graded with azimuthal uniformity
Sky Type 4	Overcast moderately graded and slight brightening towards the sun
Sky Type 5	Overcast, foggy or cloudy with overall uniformity
Sky Type 6	Partly cloudy with a uniform gradation and slight brightening towards the sun
Sky Type 7	Partly cloudy with a brighter circumsolar effect and uniform gradation
Sky Type 8	Partly cloudy, rather uniform with a clear solar corona
Sky Type 9	Partly cloudy with a shaded sun position
Sky Type 10	Partly cloudy with brighter circumsolar effect
Sky Type 11	White-blue Sky with a clear solar corona
Sky Type 12	Very clear/unturbid with a clear solar corona
Sky Type 13	Cloudless polluted with a broader solar corona
Sky Type 14	Cloudless turbid with a broader solar corona
Sky Type 15	White-blue turbid Sky with a wide solar corona effect

Methods

The research is divided into three separate sub-activities. The first activity concentrates on the CIE analysis of the raw luminance data acquired from the installed sky scanner apparatus at the MTCoE facility in Gurugram, India. A box model as shown in Fig. 1 was developed, and a daylight simulation was performed using VELUX daylight visualizer software to extract illuminance levels for a correlation analysis of recorded CIE sky conditions with overcast sky conditions as the second activity of the study. The model was set up in VELUX Daylight Visualizer 3.0 to simulate daylighting for two years on March 21 and September 21 for 900, 1200, 1500, and 1800 hrs. A 54 square meter office space with a 25% window-to-wall area ratio (WWR%), transparent glass with a visible light transmittance (VLT) of 51%, and surfaces with surface reflectance of 21% for the floor, 74% for the ceiling, and 51% for the walls makes up the simulation base case. The last activity involves applying the coefficient of correlation approach to compare the observed Sky with the default overcast state. The run chart for the used method is shown in Fig. 2.

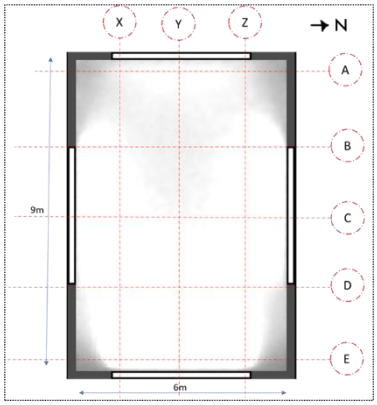

Figure 1: Box Model

Activity-1 CIE Analysis of Luminance Distribution Data

Using the extracted luminance distribution data from the sky scanner equipment and the root mean square error (RMSE) adopted from ISO 15469:2004 [9], the performance of each CIE standard sky luminance model was assessed twice a year on 21st of March and September. The studied CIE sky types are illustrated in Fig. 3-4, which are also utilized as input for Activity-2 sky-type consideration for CIE-measured sky simulations.

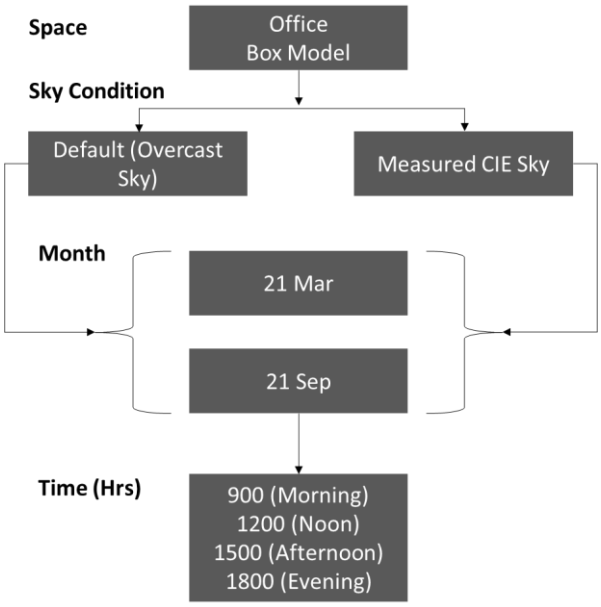

Figure 2: Simulation Methodology-Run Chart

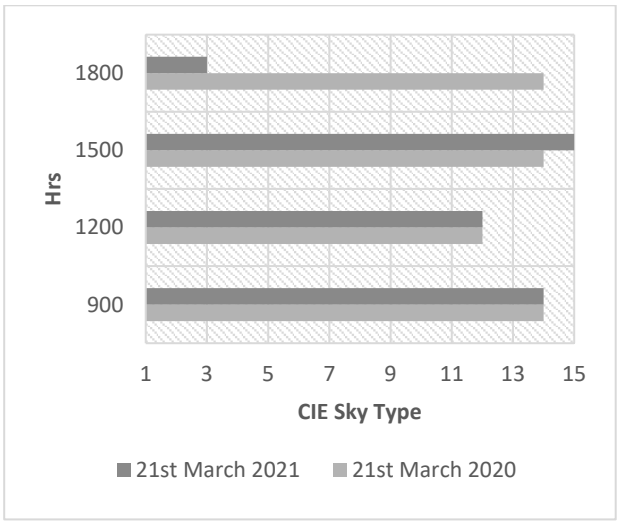

Figure 3: CIE Sky Type for March

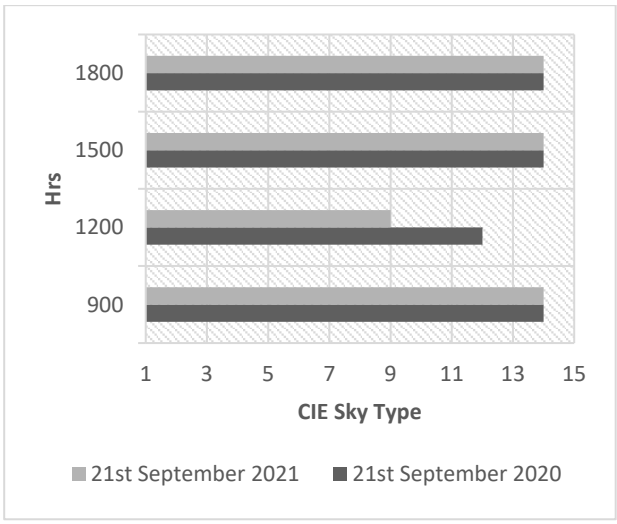

Figure 4: CIE Sky Type for September

Activity-2 Daylight Simulations

To run the daylight simulations under the CIE overcast sky type and the CIE observed sky type from the study of Activity-1, a 3D model was developed. The VELUX daylight visualizer 3.0 software enables users to do daylight simulations, considering any sky condition of the CIE 15 general sky type for the 21st of March and September. The analyses of the daylight simulation are illustrated in Fig. 5 to 12. The analyzed measured CIE sky-type, and default conditions in lux are shown in Table II to V, which is further used as an input for sky type consideration for CIE-measured sky simulations as described in Activity-3.

TABLE II. MARCH 21, 2020, OVERCAST CONDITIONS AND MEASURED CONDITIONS

		Default Sky (lux)			Measured Sky (lux)		
900	**Points**	**X_d**	**Y_d**	**Z_d**	**X_m**	**Y_m**	**Z_m**
	A	1315	1664	1208	1046	1304	1040
	B	583	526	693	1338	1125	1486
	C	716	493	928	1411	1219	1465
	D	617	532	723	1768	2044	1639
	E	1502	1556	1299	2913	2982	2716
1200	**A**	1686	2381	1658	1119	1335	1004
	B	961	770	876	952	913	1232
	C	1097	723	1142	1128	906	1378
	D	930	739	949	1082	1067	1109
	E	1978	2337	2050	3007	3282	2892
1500	**A**	1238	1497	1111	2943	2661	1740
	B	677	546	609	1716	2095	1670
	C	833	498	827	1610	1271	1478
	D	702	521	676	1435	1127	1397
	E	1411	1675	1335	1012	1356	1135
1800	**A**	60	82	58	325	343	178
	B	37	27	31	336	359	307
	C	43	25	40	324	319	301
	D	35	26	34	259	235	309
	E	70	84	71	311	295	249

TABLE III. MARCH 21, 2021, OVERCAST CONDITIONS AND MEASURED CONDITIONS

		Default Sky (lux)			Measured Sky (lux)		
	Points	**X_d**	**Y_d**	**Z_d**	**X_m**	**Y_m**	**Z_m**
	A	1315	1664	1208	1046	1304	1040
900	**B**	583	526	693	1338	1125	1486
	C	716	493	928	1411	1219	1465
	D	617	532	723	1768	2044	1639

	E	1502	1556	1299	2913	2982	2716
	A	1686	2381	1658	1119	1335	1004
	B	961	770	876	952	913	1232
1200	**C**	1097	723	1142	1128	906	1378
	D	930	739	949	1082	1067	1109
	E	1978	2337	2050	3007	3282	2892
	A	1238	1497	1111	2412	2913	1840
	B	677	546	609	1709	2207	1537
1500	**C**	833	498	827	1514	1217	1652
	D	702	521	676	1323	1114	1508
	E	1411	1675	1335	1166	1282	1127
	A	60	82	58	449	511	469
	B	37	27	31	591	662	541
1800	**C**	43	25	40	523	466	486
	D	35	26	34	478	429	495
	E	70	84	71	480	493	483

TABLE IV. SEPTEMBER 21, 2020, OVERCAST CONDITIONS AND MEASURED CONDITIONS

		Default Sky (lux)			**Measured Sky (lux)**		
	Points	**X_d**	**Y_d**	**Z_d**	**X_m**	**Y_m**	**Z_m**
	A	1349	1872	1272	3053	3745	2332
	B	773	624	759	2841	2396	2887
900	**C**	1077	565	977	3139	2392	3264
	D	796	611	724	2771	2785	2838
	E	1543	1938	1672	4915	5728	5165
	A	2140	2594	1923	1023	1253	1016
	B	1019	843	1008	1152	851	940
1200	**C**	1305	789	1467	1314	870	1196
	D	1023	837	1023	991	994	994
	E	2100	2656	2144	2439	2859	2641
	A	1396	1860	1389	2776	3990	3455
	B	811	609	764	1177	1590	1490
1500	**C**	1046	576	905	1744	1031	1261
	D	777	608	737	1478	970	1044
	E	1502	1901	1648	953	1107	1044
	A	103	162	96	1136	1389	1139
	B	71	54	63	893	1240	1041
1800	**C**	91	50	85	934	881	929
	D	63	55	62	880	783	839
	E	137	169	143	780	855	884

TABLE V. SEPTEMBER 21, 2020, OVERCAST CONDITIONS AND MEASURED CONDITIONS

		Default Sky (lux)			**Measured Sky (lux)**		
	Points	**X_d**	**Y_d**	**Z_d**	**X_m**	**Y_m**	**Z_m**
	A	1349	1872	1272	3053	3745	2332
	B	773	624	759	2841	2396	2887
900	**C**	1077	565	977	3139	2392	3264
	D	796	611	724	2771	2785	2838
	E	1543	1938	1672	4915	5728	5165
	A	2140	2594	1923	2929	4774	3722
	B	1019	843	1008	4759	3441	3736
1200	**C**	1305	789	1467	6671	3425	4270
	D	1023	837	1023	4191	3832	4270
	E	2100	2656	2144	4387	8012	7417
	A	1396	1860	1389	2776	3990	3455
	B	811	609	764	1177	1590	1490
1500	**C**	1046	576	905	1744	1031	1261
	D	777	608	737	1478	970	1044
	E	1502	1901	1648	953	1107	1044
	A	103	162	96	1136	1389	1139
	B	71	54	63	893	1240	1041
1800	**C**	91	50	85	934	881	929
	D	63	55	62	880	783	839
	E	137	169	143	780	855	884

Activity-3 Comparison of Default Sky with Measured Sky

Actual observations of daytime illuminance levels from Activity-1 were contrasted with simulations of the same values from Activity-2. The association between two variables is described using the correlation coefficient approach. The dependability of the line generated is shown by how well the best-fit line corresponds to the sample data, which is determined by the Pearson correlation coefficient. The Pearson correlation coefficient ranges from 1 to 0, with 1 denoting a perfect connection. The below equation is used to find the Pearson correlation coefficient (r).

$$r = \frac{\Sigma(x - \bar{x})(y - \bar{y})}{\sqrt{\Sigma(x - \bar{x})^2 \, \Sigma(y - \bar{y})^2}}$$

where x, y are the x and y values of default and measured Sky, and x, y are the average of x and y values default and measured Sky.

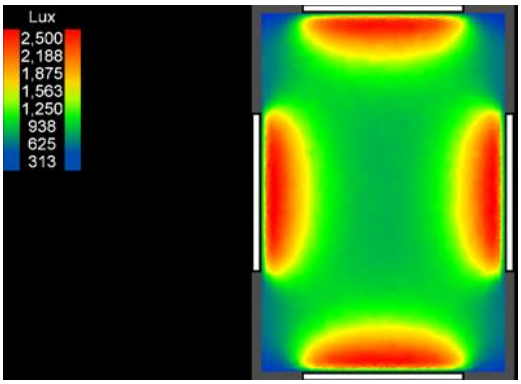

Figure 5: Default Sky March 21 2021 -1200 hrs

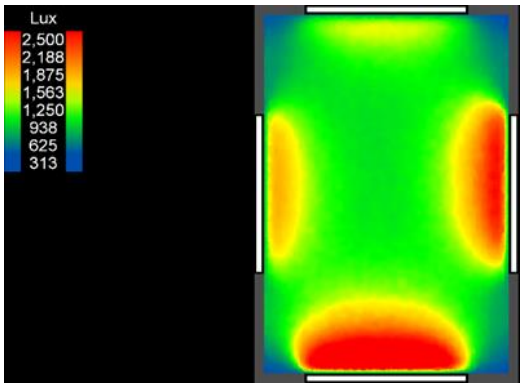

Figure 6: Measured Sky March 21 2021 -1200 hrs

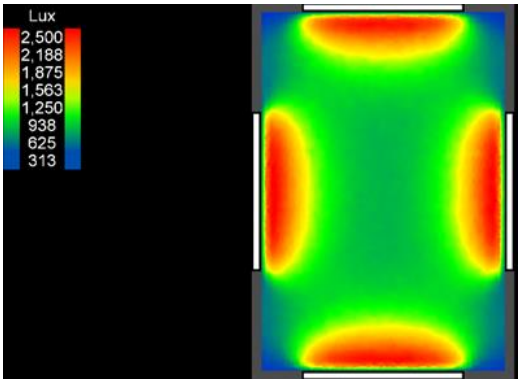

Figure 7: Default Sky March 21 2021 -1200 hrs

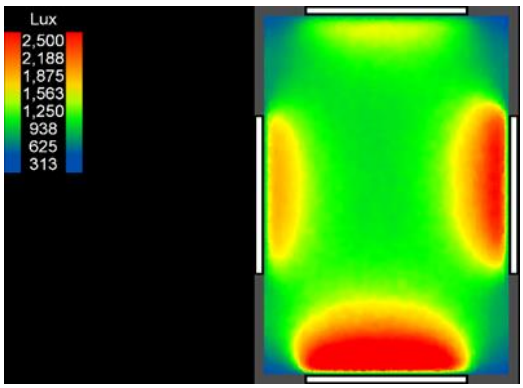

Figure 8: Measured Sky March 21 2021 -1200 hrs

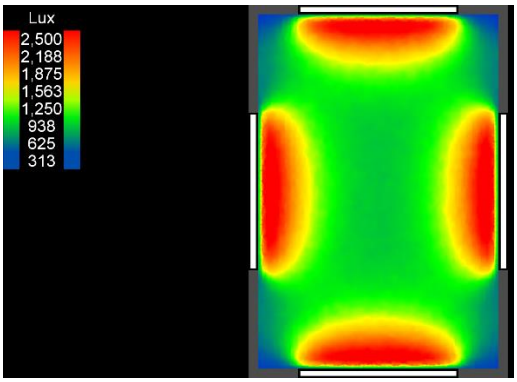

Figure 9: Default Sky September 21 2020 -1200 hrs

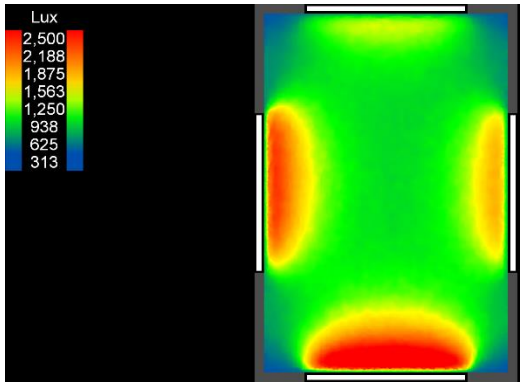

Figure 10: Measured Sky September 21 2020 -1200 hrs

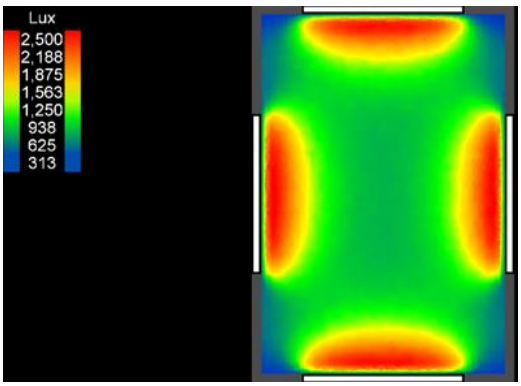

Figure 11: Default Sky March 21 2021 -1200 hrs

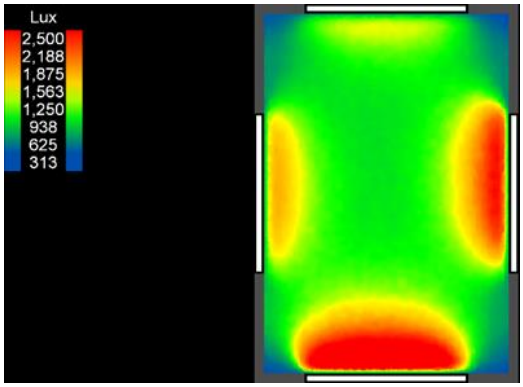

Figure 12: Measured Sky March 21 2021 -1200 hrs

Results & Discussions

According to analysis using the Pearson correlation coefficient, recorded sky condition levels were 38 to 49% more accurate on March 21, 2020, at 900 hours than overcast sky-type illuminance; a similar pattern was observed on March 21, 2021. At 900 hours in September 2020 and September 2021, measured sky conditions were 70 to 88% more accurate than the illuminance level of an overcast sky. According to Fig. 3-4, the primary sky type at 900 hours is CIE sky type 14, which is cloudless turbid with a wider sun corona. Fig. 13-14 illustrate correlation between overcast and measured sky conditions at 900 hours for 21st of March and September.

TABLE VI. COMPARISON OF CORRELATION COEFFICIENT OF OVERCAST SKY VS MEASURED SKY

	X_d vs X_m	Y_d vs Y_m	Z_d vs Z_m
900 hrs			
21st March 2020	49%	43%	38%
21st March 2021	49%	43%	38%
	X_d vs X_m	Y_d vs Y_m	Z_d vs Z_m
21st Sep 2020	80%	88%	70%
21st Sep 2021	80%	88%	70%
1200 hrs			
	X_d vs X_m	Y_d vs Y_m	Z_d vs Z_m
21st March 2020	79%	72%	72%
21st March 2021	79%	72%	72%
	X_d vs X_m	Y_d vs Y_m	Z_d vs Z_m
21st Sep 2020	53%	76%	71%
21st Sep 2021	-49%	81%	63%
1500 hrs			
	X_d vs X_m	Y_d vs Y_m	Z_d vs Z_m
21st March 2020	11%	36%	-45%
March 21 2021	12%	34%	-36%
	X_d vs X_m	Y_d vs Y_m	Z_d vs Z_m
21st Sep 2020	26%	56%	32%
21st Sep 2021	26%	56%	32%
1800 hrs			
	X_d vs X_m	Y_d vs Y_m	Z_d vs Z_m
21st March 2020	27%	16%	-73%
21st March 2021	-56%	-9%	-66%
	X_d vs X_m	Y_d vs Y_m	Z_d vs Z_m
21st Sep 2020	-15%	29%	-10%
21st Sep 2021	-15%	29%	-10%

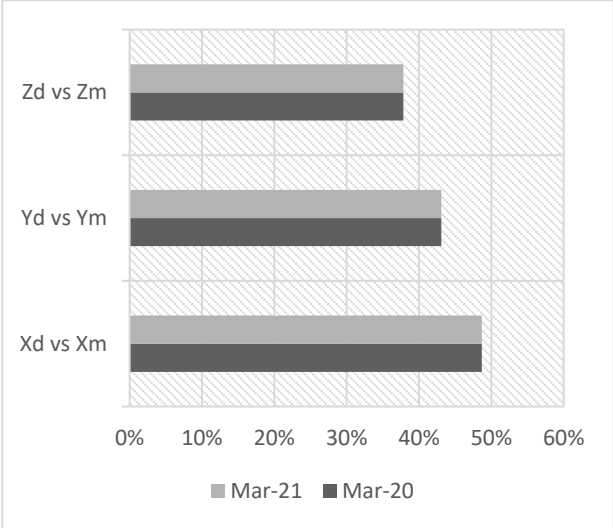

Figure 13: Correlation between overcast and measured sky conditions at 900 hrs for March

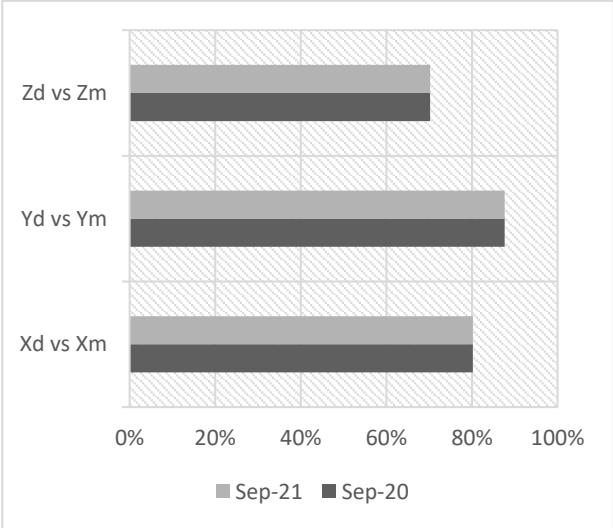

Figure 14: Correlation between overcast and measured sky conditions at 900 hrs for September

The measured sky type were found to be 72% to 79% more accurate than overcast sky type as observed at 1200 hours on March 21, 2020; for the following year, a similar trend was observed with the same precision at 1200 hours. According to Fig. 3-4, the primary sky type at 1200 hours is CIE sky type 12, which is very clear/unturbid with a clear solar corona; however, on September 21 2021, the predominant sky type is 9, which is partly cloudy with the obscured sun. At 1200 hours in September 2020, the measured sky conditions were 53% to 71% more accurate than the illuminance level of an overcast sky; however, the accuracy range changed the next year from -49% to +81%. The tremendous difference in the range was observed because the default sky remains the same for both the years and sky type changes according to the actual conditions, however, 75 % of the time, the sky pattern is of sky type 12. Fig. 15-16 illustrate correlation between overcast and measured sky conditions at 1200 hours for 21st of March and September.

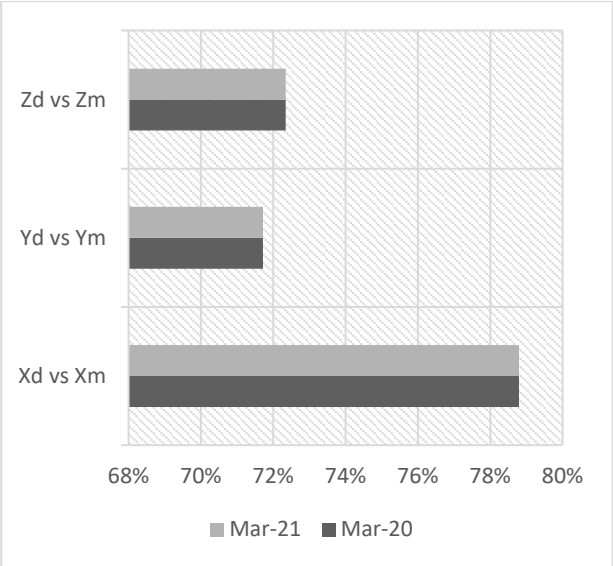

Figure 15: Correlation between overcast and measured sky conditions at 1200 hrs for March

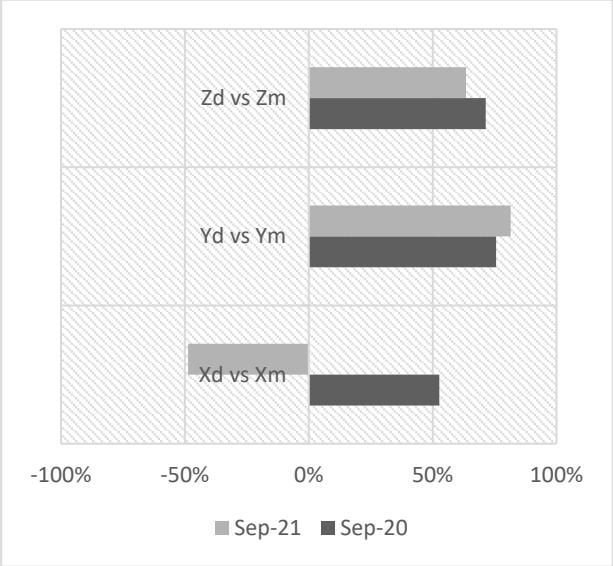

Figure 16: Correlation between overcast and measured sky conditions at 1200 hrs for September

The measured sky type was found to be in the range of -45 to +36% as compared with overcast sky type as observed at 1500 hours on March 21, 2020; for the following year, a similar trend was observed. The sky pattern for March 2021 is in negative for the same reason as previously indicated. The measured sky conditions were 26 to 56% more accurate at 1500 hours in September 2020 and September 2021 than the illuminance level of an overcast sky. The primary sky type at 1500 hours, as shown in Fig. 3-4 is CIE sky type 14, cloudless turbid with a broader sun corona. Fig. 17-18 illustrate correlation between overcast and measured sky conditions at 1500 hours for 21st of March and September.

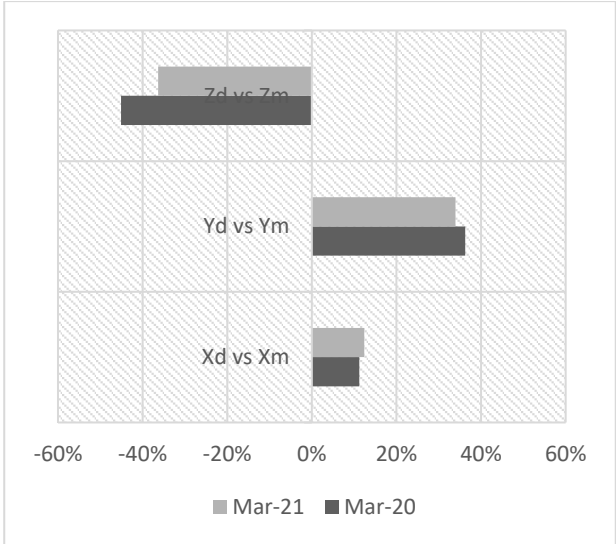

Figure 17: Correlation between overcast and measured sky conditions at 1500 hrs for March

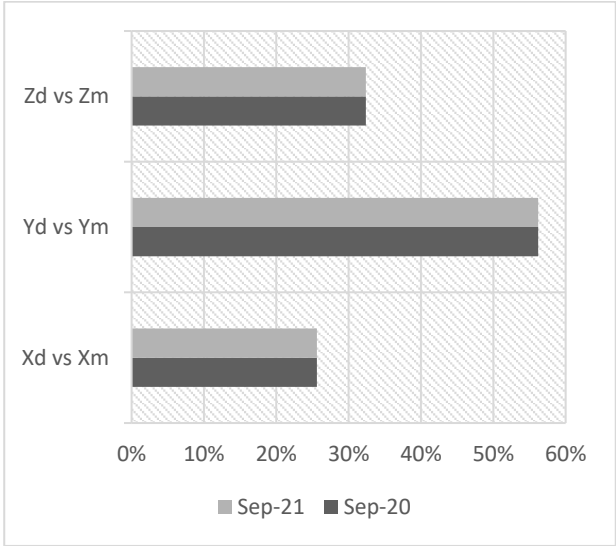

Figure 18: Correlation between overcast and measured sky conditions at 1500 hrs for September

At 1800 hours on March 21, 2020, the measured sky type was found to be in the range of -73 to +27% as compared with overcast sky type. In 2021, the correlation was found to be negative at 1800 hours. The measured sky conditions were found to be in the range of -10 to 29% % as compared with overcast sky type at 1800 hours in September 2020 and September 2021 than the illuminance level of an overcast sky. The dominant sky type at 1800 hours, as shown in Fig. 3-4 is CIE sky type 14, cloudless turbid with a broader sun corona. The average correlation for 21st of March under an overcast sky and the measured Sky was determined to be more accurate, 27% for 2020 and 19% for 2021. It was found to be more accurate on September 21, with 46% for 2020 and 38% for 2021 under the measured and cloudy Sky. Fig. 19-20 illustrate correlation between overcast and measured sky conditions at 1800 hours for 21st of March and September.

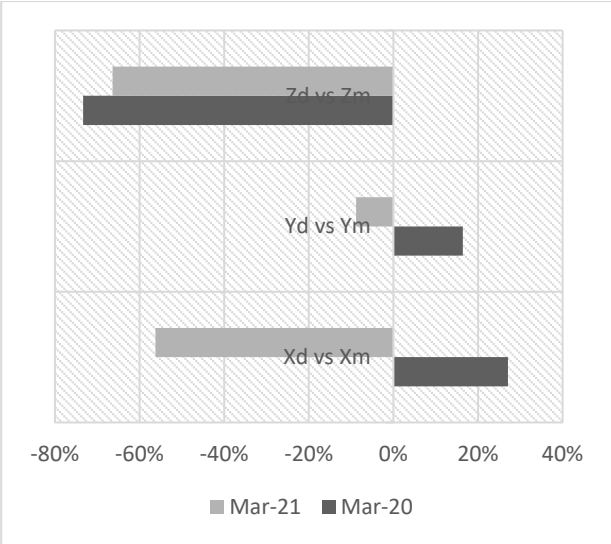

Figure 19: Correlation between overcast and measured sky conditions at 1800 hrs for March

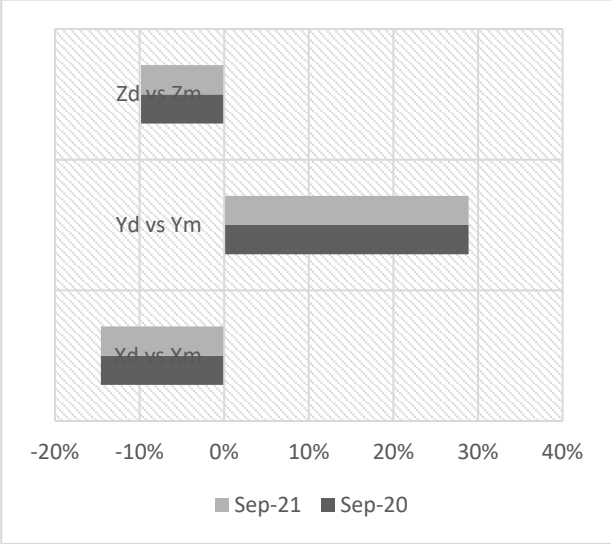

Figure 20: Correlation between overcast and measured sky conditions at 1800 hrs for September

Conclusion

The illuminance analysis perceived by daylight simulation taking into account actual sky condition compared to overcast sky condition, i.e., default sky condition considered in general practice for computing lux levels on the analysis grid, is calculated to be 27% and 19% more accurate in the months of March 2020 and 2021, respectively. This conclusion is drawn from the correlation analysis of two-year data. According to the data, the accuracy for September increased to 46% and 38% for 2021 and 2021, respectively.

The findings also show that the predominant sky type for the Gurugram location is CIE sky type 14, which is cloudless turbid with a wider solar corona. For improved illuminance prediction, the calculated set of CIE design sky may be utilized to optimize passive window design for places lying under the appropriate climatic zones.

Acknowledgements

The authors would like to thank Mahindra Lifespace for supporting and providing financial assistance for the study, Ms Shabnam Bassi, Dy. CEO, GRIHA Council and Dr Rana Veer Singh, Associate Fellow, TERI, for their suggestions and Mr Bhushan Sharma, Technical Assistant, TERI, for data accumulation.

References

[1] Danny H.W. Li, Ernest K.W. Tsang, An analysis of daylighting performance for office buildings in Hong Kong, Building and Environment, Volume 43, Issue 9, 2008, Pages 1446-1458, ISSN 0360-1323.

[2] Danny H. W. Li, Chris C. S. Lau & Joseph C. Lam (2004) A Simplified Procedure Using Daylight Coefficient Concept for Sky Component Prediction, Architectural Science Review, 47:3, 287-294.

[3] Y. K. T. M. H. N. Norio Igawa, "Models of sky radiance distribution and sky luminance distribution," *Solar Energy*, vol. 77, no. 2, pp. 137-157, 2004.

[4] D. B. T. A. K. B. S. K. Samiha Boucherit, "Analyzing the Luminous Environment in a University Campus in Biskra, Algeria: A Pilot Study," in *IOP conference series: Earth and Environmental Science*, Vienna, Austria, 2021.

[5] International Energy Agency, "Daylight in Buildings: A Source Book on Daylighting Systems and Components," 2000.

[6] Tregenza P. Mean daylight illuminance in rooms facing sunlit streets. Building and Environment 1995;30: 83–9.

[7] Tsangrassoulis A, Santamouris M. Numerical estimation of street canyon albedo consisting of vertical coated glazed facades. Energy and Buildings 2003; 35:527–31.

[8] J. A. O. O. J. L. Paul Kenny, "Whole-Sky Luminance Maps from Calibrated Digital Photography," in *EuroSun Conference (CD)*, Glasgow, Scotland, 2006.

[9] International Standardisation Organisation, CIE S 011/E:2003, Spatial Distribution Daylight-CIE Standard General Sky, 2004. ISO Standard 15469: 2004, Geneva.

[10] R. K. Stanislav Darula, "CIE general sky standard defining luminance distributions," in *The Canadian conference on building energy simulation (eSim)*, Montreal, Canada, 2002.

[11] R. K. Stanislav Darula, "Sunshine duration and daily courses of Illuminance in Bratislava," *International Journal of Climatology*, vol. 24, no. 14, pp. 1777-1783, 2004.